Accepted Manuscript

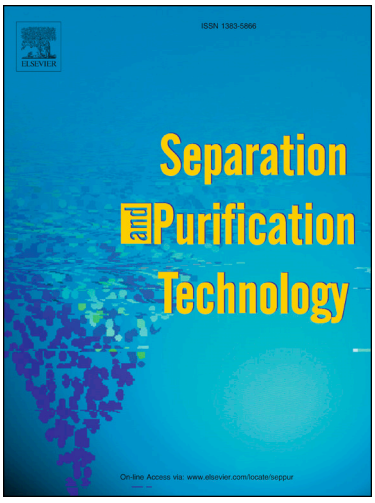

Electro-concentration for chemical-free nitrogen capture as solid ammonium bicarbonate

Johannes Jermakka, Emma Thompson Brewster, Pablo Ledezma, Stefano Freguia

PII: S1383-5866(17)34075-3
DOI: https://doi.org/10.1016/j.seppur.2018.04.023
Reference: SEPPUR 14519

To appear in: *Separation and Purification Technology*

Received Date: 11 December 2017
Revised Date: 6 April 2018
Accepted Date: 6 April 2018

Please cite this article as: J. Jermakka, E. Thompson Brewster, P. Ledezma, S. Freguia, Electro-concentration for chemical-free nitrogen capture as solid ammonium bicarbonate, *Separation and Purification Technology* (2018), doi: https://doi.org/10.1016/j.seppur.2018.04.023

Electro-concentration for chemical-free nitrogen capture as solid ammonium bicarbonate

Authors: Johannes Jermakka[1], Emma Thompson Brewster[2], Pablo Ledezma[3], Stefano Freguia[4]

[1]Corresponding author. Email: johannes.jermakka@tut.fi. Work conducted at Advanced Water Management Centre, The University of Queensland, Australia, and Laboratory of Chemistry and Bioengineering, Tampere University of Technology, Finland. Permanent address: Tampere University of Technology, Laboratory of Chemistry and Bioengineering, PO Box 541, 33101 Tampere, Finland.

[2]Email: emmathompsonbrewster@gmail.com. Advanced Water Management Centre, The University of Queensland, Australia

[3]Email: p.ledezma@awmc.uq.edu.au. Advanced Water Management Centre, The University of Queensland, Australia

[4]Email: s.freguia@awmc.uq.edu.au. Advanced Water Management Centre, The University of Queensland, Australia

Declarations of interest: none

Abstract

Source-separated urine is a promising stream for nutrient capture using electrochemical technologies. It contains the majority of macronutrients present in municipal wastewater in a concentrated, high ionic conductivity liquid and in N:P:K ratios suitable for agricultural application. The purpose of this study was to recover nutrients from urine, and particularly nitrogen as a solid without any chemical addition. Simulated source-separated urine was concentrated using a three-compartment electrochemical system, applying a range of current densities and feed compositions. Electro-concentration into a liquid concentrate reached maximum recovery of 72:61:79 % for N:P:K, respectively, from a synthetic feed simulating ureolysed and digested urine, with a specific electrical energy consumption of 47 MJ/kg N and current efficiency of 67 % for ammonium. Cooling the concentrate to -18°C resulted in solid ammonium bicarbonate crystal formation in samples with high ammonium bicarbonate ionic product and high relative ammonium bicarbonate ionic strength. Precipitation started to occur when ammonium bicarbonate ionic product was higher than 2.25 M^2 and ammonium bicarbonate accounted for more than 62 % of the total ionic strength of the feed. The maximum observed nitrogen recovery into solid ammonium bicarbonate reached 17 % using a current density of 100 A m^{-2}. Based on these results, electro-concentration is a promising technology for urine nutrient capture. However, capture as solid ammonium bicarbonate is feasible only if higher recovery efficiencies are achieved by removing competing ions.

Keywords: nutrient recovery; urine; electro-concentration; ammonium bicarbonate precipitation

1 Introduction

Source-separated, decentralized systems offer promising alternatives for the future of human sanitation enabling localised recovery of nutrients and water resources [1]. While planetary boundaries of Earth are under unprecedented stress by population growth and climate change [2],

source separation can provide means of reducing community energy and water consumption by enabling water and nutrient recovery and reuse, even in situations of inadequate infrastructure [1]. Of source-separated domestic wastewater streams, greywater contains most of the recoverable water. Faecal matter (0.1 % of wastewater stream) in turn contains most of the organic loading and almost all pathogens, while urine contains the majority of nutrients (79-47-71 % and 86-65-76 % of N:P:K in total domestic wastewater and excreta, respectively) [3]. This renders source-separated urine the most promising domestic stream for nutrient recovery [4].

Nutrients in urine are typically found in ratios suitable for direct reuse as fertiliser [5] but, while use of human urine for agriculture is well known, direct reuse is not always feasible due to liquid transportation costs, handling, salinity and health and safety issues [6]. However, technologies enabling recovery of nutrients from source-separated urine as separate streams are not widely applied [7]. Phosphorus is the most studied nutrient for recovery from source-separated urine, typically captured as solid struvite precipitate [8–11], while no references for selective potassium recovery are found. Nitrogen capture from urine has been studied through several methods including stripping [12,13], electrodialysis [14–16], electro-concentration [17–19] and microbial electrochemical technologies (METs) [20–24]. Nitrogen recovery as solid ammonium bicarbonate without chemical addition has been proposed by means of a combined microbial electrochemical cell and electro-concentration [25].

Urine is an excellent feed for electrochemical treatment being (i) highly conductive, avoiding Ohmic losses problematic in normal sewage, (ii) well buffered, enabling operation with low pH differences and thus lower thermodynamic voltage requirements between anode and cathode, (iii) and highly concentrated in nutrients [4]. For instance, electrodialysis of human urine was studied by Pronk et al. (2006b) reaching high degrees of desalination (e.g. N, P and K recoveries of 93, 74 and 94 %, respectively). Electrodialysis was further studied with alternative settings with a membrane contactor ammonium capture device [26] and also in pilot scale [27]. Electrodialysis has similarly been applied for nitrogen recovery from a similar waste stream, swine manure [28,29]. Also, electro-concentration using a two chamber electrochemical cell has been studied for ammonium removal and recovery from anaerobic digestate, enabling reasonable ammonium capture at low energy consumption measured approximately 18 - 150 MJ/kg N [18,19]. The same technology has been applied also for human urine [15,17], with subsequent ammonia stripping measured at 43 MJ/kg N. A similar three-cell system, as used in this article, has been used to model and evaluate the limiting factors of electro-concentration [30]. These studies demonstrate that electro-concentration is technically feasible and also an economically promising solution for different feeds.

Most of the aforementioned nitrogen-specific technologies use ammonia gas stripping followed by capture into strong acid solutions (*e.g.* sulfuric acid). This is effective, but the use of strong acids is a disadvantage adding to the cost and risk of operation, especially in decentralized scenarios.

Sufficiently concentrated urine has the potential to become saturated in ammonium bicarbonate when cooled, as the solubility of ammonium bicarbonate reduces with temperature. This can induce precipitation of solid ammonium bicarbonate crystals allowing for chemical free recovery of nitrogen as a solid [25]. Precipitation of ammonium bicarbonate from concentrated urine is not widely discussed in the literature. It is highly soluble (17.6 g/100g H_2O at 20°C [31]) but its actual solubility in high strength salt solutions, such as urine, is unknown as generalised wastewater physico-chemical speciation models do not exist for solutions with many components and high ionic strength [30]. Other species with similar range solubilities include potassium bicarbonate and sodium bicarbonate (24.9 and 8.7 g/100g H_2O at 20°C, respectively [31]). As temperature is lowered, the solubility of ammonium bicarbonate decreases relatively more than other bicarbonates (10.6, 18.6

and 6.5 g/100g H_2O at 0°C for ammonium, potassium and sodium bicarbonate, respectively [31]). As potassium and sodium are present in lower concentrations in urine to ammonium, ammonium bicarbonate is expected to precipitate first when urine is cooled. Commonly used speciation models such as PHREEQC 3 and Visual MINTEQ 3.1 do not currently extend to highly concentrated solutions such as concentrated urine [30], and experimental results are required to confirm this hypothesis.

In this paper, changes in urine concentrate composition correlating to the feed composition and the applied current density are demonstrated by means of a three compartment abiotic electro-concentration cell fed with synthetic urine. Inspired by a bio-electrochemical concept demonstrated by Ledezma et al. [25], the abiotic approach allows rapid mapping of parameters beyond the limitations of microbiological constraints. Synthetic urine was chosen to enable consistency when systematically varying the experimental factors of applied current density and feed composition [32,33]. Nitrogen recovery is achieved as solid ammonium bicarbonate via cooling, and the limits for recovery as a solid are identified.

2 Materials and methods

2.1 Medium composition

A synthetic urine solution (referred to as ACE as it contains acetate as representative of the organic fraction) representing ureolysed urine was selected based on work done at the Swiss Federal Institute of Aquatic Science and Technology (EAWAG) [33,34] consisting of (g L^{-1}) Na_2SO_4 (2.3), NaH_2PO_4 (2.1), NaCl (3.6), KCl, (4.2), $NH_4CH_3CO_2$ (9.6), NH_4OH (25 % liquid, 13mL L^{-1}), NH_4HCO_3 (21.4). This recipe simulates urine after complete removal of Mg and Ca through precipitation with phosphate during ureolysis, and models organic content with acetate. A composition without ammonium acetate was tested (referred to as NO ACE) identical to ACE, except without addition of $NH_4CH_3CO_2$. A further medium was developed in which all acetate was assumed to be digested into carbon dioxide, modelling fully digested ureolysed urine. This digested urine recipe (referred to as ABC for ammonium bicarbonate) consisted of g L^{-1}) Na_2SO_4 (2.3), NaH_2PO_4 (2.1), NaCl (3.6), KCl, (4.2), NH_4OH (25 % liquid, 3.5mL L^{-1}), NH_4HCO_3 (41.2). The feeds were prepared as used and feed composition was monitored through sampling when changing the feed. Synthetic urine was chosen to enable consistency when systematically varying the experimental factors.

2.2 Reactor and equipment

Custom reactors were used consisting of three acrylic plates forming three parallel compartments (anodic, middle and cathodic) of 70 mm x 50 mm x 10 mm each (see Figure 1). Four identical reactors were used as replicates. The anodic compartment was filled with a packed bed of acid and alkaline washed graphite granules (granule size 2 - 10 mm; EC-100, Graphite Sales Inc., USA,) with a graphite rod (Ø5 mm; Element14, Australia) acting as a current collector. The anode was separated from a middle compartment by a Cation Exchange Membrane (CEM) (CMI-7000 Membrane International Inc., USA). The cathodic compartment contained a 70 mm x 50 mm stainless steel mesh as a cathode and was separated from the middle compartment by an Anion Exchange Membrane (AEM) (Membrane International Inc. AMI-7001). The projected surface area of both membranes and electrodes was 35 cm^2 and the volume of each chamber was 35 mL, rendering the reactor effective volume as 105 mL. The anodic and cathodic compartments were hydraulically connected forming a loop including an online pH meter (Endress+Hauser Liquisys CPM253) and a circulation pump. The middle compartment was connected to an overflow bottle with a gas bag and was not open to the atmosphere. A potentiostat (Bio-Logic VMP-3) was used as a power source in two electrode mode, applying constant current and recording the voltage applied and electrical energy used. Current densities of 40 to 100 A m^{-2} were applied. A cooling coil system (RC1, Ratek, Australia) was used to

lower the temperature of a thermally-isolated container to +4°C to store the collected concentrate. A freezer set to -18°C was used to cool the collected concentrate.

2.3 Operation

Feed was pumped into each reactor at a constant rate of 20.9 ± 0.4 mL h^{-1} to the anodic chamber of the reactor. The anodic chamber and the cathodic chamber were connected and constantly circulated at 2100 mL h^{-1}. Effluent was collected from the cathodic chamber. A concentrate was formed as the middle chamber overflow and was collected into a 250 mL bottle kept at 4°C. Flow schematics are presented in Fig 1a. A constant current density, J [A m^{-2}], between the electrodes was applied and the voltage required for this current was logged by the potentiostat. All runs were initiated with feed in all compartments and monitored until steady state was reached and no change in composition in the middle chamber was detected. All experimental runs showed a clear concentration phase and subsequent steady state phase. Samples from three runs were analysed during the concentration phase, all other runs were sampled and analysed only during steady state - a list of experiments can be found in the results section (Table 1). In steady state operation, empty overflow collection bottles were used to collect the overflow over a set time period. 1.5 mL samples were taken from the feed, the anodic chamber, the middle chamber, and the effluent. Samples were taken at the start and end of a steady state phase. At the end of a steady state experiment, the concentrate collection bottle was removed, sampled, measured for volume and set in a freezer (-18°C). After 18 h the supernatant was filtered (0.45 µm) to separate the formed crystals and measured for volume, with precipitated solids collected for reference. The collected solids were redissolved in 2000 mL deionized water and sampled. All samples were filtered (0.45 µm) and diluted with deionized water for analysis. Results presented with 95 % confidence intervals represent parallel results from repeated experiments. Repetitions were done 1, 2 or 4 times, depending on the experiment (see Table 1).

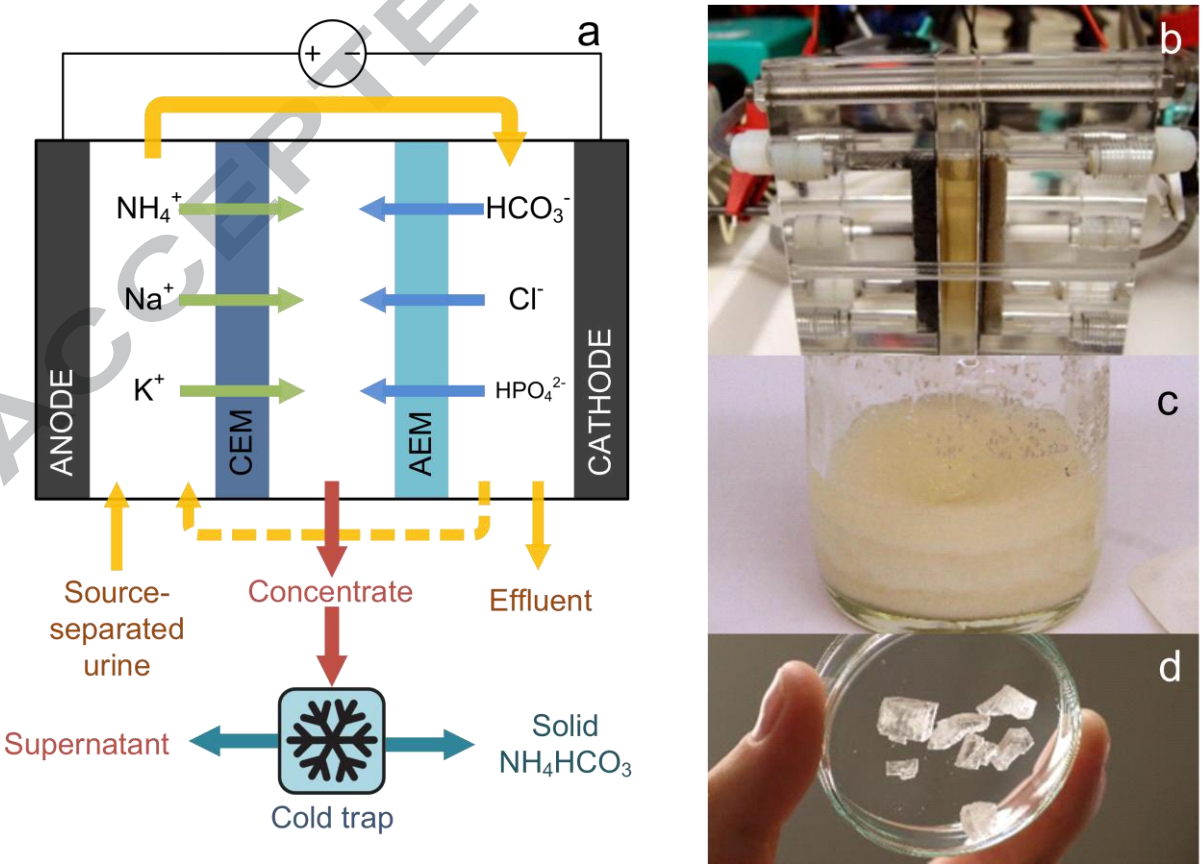

Figure 1. Experiment illustrations. a) Schematic flow chart, (b) Three compartment reactor, (c) precipitated solids after cooling and decanting, and (d) air dried solid ammonium bicarbonate crystals from the precipitated solids. CEM: cation-exchange membrane. AEM: anion-exchange membrane.

2.4 Sample analysis

Samples were analysed for pH, conductivity (EC), chloride and TAN (Total Ammonium Nitrogen) with Horiba B-712 pH meter, Horiba B-771 EC meter, Merck Spectroquant Chloride Test (101807), and Merck Spectroquant Ammonium Test (114752), respectively. These results confirmed the formation of steady state conditions and ruled out leaks or other problems. Samples from three concentration stages and 13 steady state samples were further analysed, respectively, for elemental analysis, ammonia species, anions and carbon species using Inductively Coupled Plasma Optical Emission Spectroscopy (ICP-OES) (Perkin Elmer Optima 7300DV, Waltham, MA, USA) after nitric acid digestion (calcium, sodium, potassium, magnesium); Flow Injection Analysis (FIA) Lachat QuickChem8500 (Lachat Instruments, Loveland, CO, USA); Ion Chromatography Dionex ICS-2100 (Dionex, CA, USA); and Total Organic Carbon Analyser Shimadzu TOC-L CSH with TNM-L TN unit (Kyoto, Japan).

Raman spectroscopy was taken from sample of formed crystals employing an Alpha 300 (WITec GmbH, Ulm, Germany) equipped with a 40x collar corrected (Nikon) objective. A frequency doubled continuous-wave Nd:YAG laser stabilized at 532 nm was used for excitation. Raman signals were collected with a 50 mm optical fibre with a resolution of 4 cm^{-1}. For all the measurements the laser power at the sample was less than 10 mW.

2.5 Calculations

Ionic strength to compare salinities of samples was calculated using equation 1.

$$IS = \frac{1}{2}\sum_{i=1}^{n} c_i z_1^2 = \frac{1}{2}([NH_4^+] + [Na^+] + [K^+] + [Cl^-] + [HCO_3^-] + [SO_4^{2-}][-2]^2 + [HPO_4^{2-}][-2]^2) \quad (1)$$

where IS is ionic strength, c_i is molarity (mol L^{-1}) and z_i is charge. No corrections for activities were applied [35].

The ionic strength of ammonium bicarbonate was calculated using equation 2.

$$IS_{ABC} = {}^1/_2\,([NH_4^+] + [HCO_3^-]) \quad (2)$$

where $[NH_4^+]$ and $[HCO_3^-]$ are ammonium and bicarbonate concentrations. This represents the share of ammonium bicarbonate of the total ionic content of the solution. Activity coefficients were assumed to be 1. This formula was mainly used to calculate the relative fraction of ammonium bicarbonate in ionic strength IS_{ABC}/IS.

Ammonium bicarbonate ionic product was calculated using equation 3.

$$IP_{ABC} = [NH_4^+][HCO_3^-] \quad (3)$$

where $[NH_4^+]$ and $[HCO_3^-]$ are ammonium and bicarbonate concentrations [36]. Activity coefficients were assumed to be 1. Ionic product is used to determine saturation of species for precipitation.

The Coulombic efficiency for ammonium transfer was calculated according to equation 4.

$$CE = \frac{n_{NH4} \times z_{NH4}}{Q \times F} \quad (4)$$

where CE is Coulombic efficiency, n_{NH4} is moles of ammonium ions transferred (mol), and z_{NH4} is charge of ammonium ion (1), Q is the charge passed by the potentiostat (C) and F the Faraday constant (96 485 C mol^{-1}) [36].

Statistical tests were conducted using MathWorks MATLAB R2017 and Microsoft Excel 2016 Data Analysis. The analysis included one-way and multivariable analysis of variance (ANOVA), and coefficients of correlation using MATLAB, and regression analysis using Microsoft Excel. A significance threshold of 5 % was used for all statistical tests and error margins given for values represent 95 % confidence intervals for all values presented.

3 Results and discussion

3.1 Concentrate strength remains similar with varied applied current and feed composition

During the concentration stage the middle compartment concentration increases as ions migrate through the ion selective membranes due to the applied potential. The consequent higher concentration gradient across the membrane increases water osmosis through the membrane. In addition, the concentration gradient causes back migration of ionic species from the middle chamber to the catholyte and anolyte due to non-ideal membrane permselectivity, and uncharged ion pairs diffuse across the ion exchange membranes, resulting in a concentration plateau of the concentrate [37]. Electro-osmosis also contributes to water flow into middle chamber [38].

Measured ionic conductivities and ionic concentrations during concentration and steady state phases are presented in Figure 2. The plateau concentrations reached for each feed and current density (J) applied are found in Table 1. No membrane fouling or scaling was detected during the duration of experiments and no difference in results was seen between runs with fresh and used membranes (results not shown).

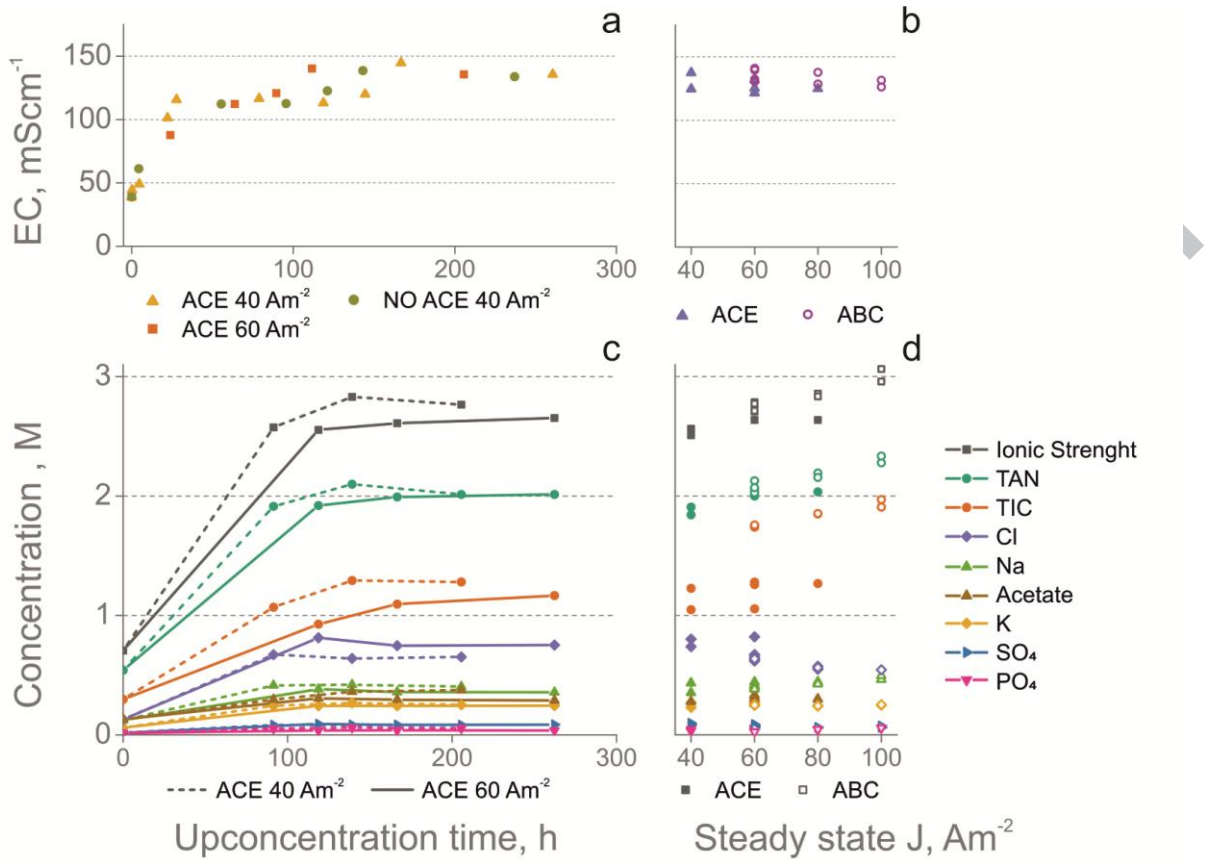

Figure 2. Concentration and steady state characteristics. a) Increase of concentrate conductivity during concentration phase. b) Concentrate conductivity in steady state for different feeds and different current densities. c) Increase of concentrate concentrations during concentration phase. d) Concentrate concentrations in steady state for different feeds and current densities. The ionic conductivity of concentrate is constant with different feeds and current densities while ionic strength and concentrations are affected by feed and current density.

In order to study the saturation in large concentrations, a speciation model is commonly used to find out activities of different species. However, high concentrations and large number of components found in our concentrate render it unsuitable for currently existing speciation models [30]. Thus saturation was studied experimentally using conductivity and measured concentrations.

As current density was increased, water flux into concentrate at steady state was found to be proportional to the current density within the studied current density range (a linear regression analysis using MS Excel fitted the model $Q_{\%} = 0.147\ \%/A\ m^{-2} \cdot J + 3.66\%$ with a p-value of 0.001, where $Q_{\%}$ is the portion of water in the feed to flow to the concentrate) (Table 2). This supports the notion that as more ions cross the membrane, more ion-bound water is transported while the higher concentration gradient also induces higher water current through osmosis.

As water flux increases, the measured ionic conductivity forms a plateau averaging 131 ± 4 mS cm^{-1} (see Figures 2a and 2b). Applied current density or feed do not affect the conductivity within the limits of the experiments considering a 5% significance threshold (one-way ANOVA using MATLAB gives p-values 0.96 and 0.20 for current density and feed, respectively).

While conductivity was unaffected by the applied current density, the ionic strength, calculated as shown in Equation 1, was observed to increase as current density J increased. Linear regression using Microsoft Excel 2016 fitted the model $IS = 0.0068\ M/A\ m^{-2} \cdot J + 2.2961\ M$ with a p-value of $1.1 \cdot 10^{-4}$, less than 5%, indicating a significant relationship (see Fig 2d). This result suggests that current density correlates with the ionic strength of the concentrate linearly within the limits of the

experiment. The increase in ionic strength observed was statistically significant but small, increasing only 16 %, while current density more than doubled from 40 to 100 A m^{-2}.

The discrepancy between plateauing of ionic conductivity and the small increase of ionic strength with current density is an interesting finding. A plausible explanation is that the proportion of chargeless species can increase with increasing concentration, thus not increasing the actual activities of charged species. As full speciation is not available, this remains a result to be verified. For single salt solutions, it has been shown that ionic conductivity can plateau and drop in high concentrations due to a larger portion of the salt remaining in non-ionic form [36]. This however typically happens only at salinities in the range of tens of percent's in mass, which were not reached here.

Considering energy efficiency during electro-concentration at different current densities, current efficiency for ammonium transport over the CEM from anode to concentrate was 63-72 % (average 67±2 %) in all experiments without a statistically significant dependence on current density or feed type (a two-factor ANOVA using MATLAB gives p-values of 0.453 and 0.169 for current density and feed, respectively).

Table 1. Feed, concentrate and filtered precipitated concentrate main ionic components. NO ACE and ABC feeds do not contain acetate. N = number of parallel experiments. If multiple experiments, values are averages with 95 % confidence intervals. All values in mM expect current density J in A m^{-2}.

Feed	J	N	TAN[1]	Na	K	TIC[2]	Cl	Acetate	SO_4	PO_4
NO ACE	**Feed**		**444**	**111**	**56**	**271**	**118**	**NA**	**16**	**18**
	40	1	1842	434	270	1226	801	NA	97	42
ACE	**Feed**		**568**	**111**	**56**	**271**	**118**	**125**	**16**	**18**
	40	1	1906	353	230	1047	739	277	83	33
	60	2	2049±20	428±21	255±11	1268±15	669±4	332	82±5	51±7
	80	1	2035	444	240	1266	550	Err[3]	62	48
ABC	**Feed**		**568**	**111**	**56**	**521**	**118**	**NA**	**16**	**18**
	60	4	2065±39	399±11	250±3	1747±8	632±12	NA	66±5	25±1
	80	2	2174±25	428±4	245±2	1852±3	568±7	NA	61±1	45±1
	100	2	2306±40	480±23	250±3	1939±45	544±1	NA	68±9	58±1
Supernatant after solids precipitation										
ABC	60	4	1606±54	429±10	253±4	1223±30	669±7	NA	69±5	28±2
	80	2	1585±140	437±1	239±1	1315±85	582±12	NA	63±1	44±2
	100	2	1817±55	500±20	250±1	1413±80	563±4	NA	71±10	61±1

[1] Total Ammonia Nitrogen, NH_4^++NH_3
[2] Total Inorganic Carbon, CO_2+HCO_3^-+CO_3^{2-}
[3] Error in sample preparation

The relative ionic concentrations for different current densities are presented in Figure 3 for the concentrate and the diluate for ACE and ABC feeds. Increase in current density increases the extent of salt removal from the feed (one-way ANOVA gives p-value of 0.0004 for current density), which is reflected in the diminishing diluate concentrations. Different ions concentrate with different ease through the membranes based on their diffusion coefficients, also referred as ion mobility. The diffusion coefficients for diffusion at infinitely small concentrations for Cl^-, K^+, NH_4^+, Na^+, HCO_3^-, $CH_3CO_2^-$ and $H_2PO_3^-$ are (in 10^{-5} cm^{-2} mol^{-1}) 2.03, 1.96, 1.96, 1.33, 1.19, 1.09 and 0.96. [31], respectively. The diffusion coefficients match the order of relative concentration for ABC feed. For ACE feed, the order at 40 A m^{-2} matches for all ions except HCO_3^-, while variation is found at higher

current densities. At low current densities, a high fraction of current goes through the membranes as ions with high mobility. At higher current densities correlating to high extent of salt removal, this effect is countered as ions with high mobility get depleted and ions with lower mobility take a larger fraction of the current. As extent of salt recovery increases towards maximum, all salts should converge towards the same concentration factor. This trend can be seen in Figure 3 for ABC feed, while not yet clearly for ACE feed.

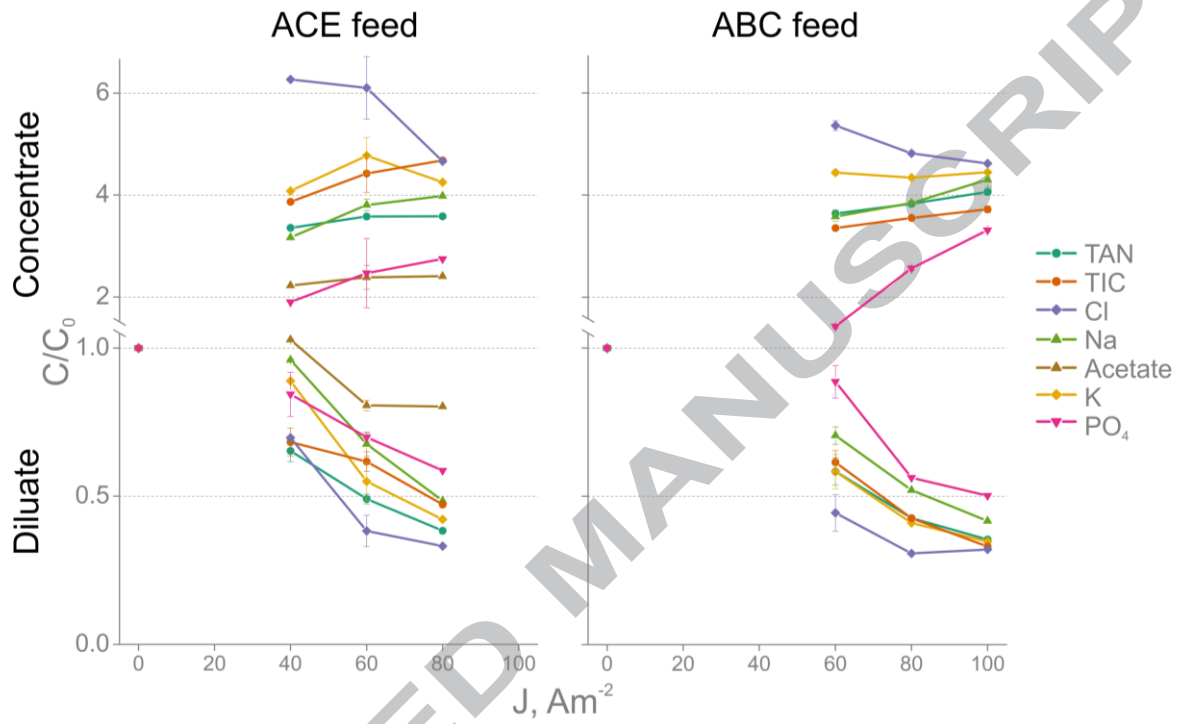

Figure 3. Relative concentrate and diluate concentrations. Synthetic ureolysed urine feed (ACE feed) and synthetic ureolysed digested urine feed (ABC feed) are presented at different current densities.

The effect of changing relative concentrations with changing current density is relatively small, but has potential for optimizing nutrient recovery technologies for targeted ions. At lower current densities (correlating to lower extent of salt removal) relatively stronger chloride and potassium concentrate can be obtained - at higher current densities relative composition converges towards feed relative composition.

3.2 Concentrate precipitation

The collected concentrate was cooled to -18 °C for 20 h, and salt precipitation occurred as mixture of small and large crystals, forming layer-like structures in runs using ABC feed. No freezing of water was observed probably due to the very high salinity. Formed crystals were identified as pure ammonium bicarbonate through Raman spectroscopy (see Figure 4) and mass balances support this observation as only ammonium and bicarbonate show significant change in liquid concentration during precipitation (see Table 1). The fractions captured in the concentrate and further in the precipitated solid are presented in Table 2. Maximum recovery rate of 72-61-79 % of N:P:K, respectively, into liquid concentrate, and 17 % recovery of N into ammonium bicarbonate solid were achieved from ABC feed at 100 A m^{-2}.

Table 2. Recovery percentage of main components and total volume into concentrate, and recovered nitrogen in subsequent solid precipitate. NO ACE and ABC feeds do not contain acetate. N = number of parallel experiments. If multiple experiments, values are averages with 95 % confidence intervals. All units in percent expect current density J in A m^{-2}.

Feed	J	N	TAN[1]	Na	K	TIC[2]	Cl	Ac	SO_4	PO_4	H_2O	Solid NH_4HCO_3[3]
NO ACE	40	1	38	33	41	37	60	NA	57	21	9.3	Not detected
ACE	40	1	33	28	37	34	55	21	47	19	9.6	Not detected
	60	2	49±2	47±2	56±2	57±1	69±1	34	66±1	39±6	12.9±0.6	Not detected
	80	1	62	63	69	74	74	Err[4]	67	47	16.4	Not detected
ABC	60	4	40±1	37±3	47±4	37±2	58±6	NA	47±6	16±1	11.4±0.3	11±1
	80	2	60±1	57±1	66±2	55±2	75±1	NA	63±2	42±2	15.7±0.4	16±4
	100	2	72±1	76±2	79±2	64±1	87±3	NA	84±9	61±2	17.8±0.6	17±3

[1] Total Ammonia Nitrogen, NH_4^++NH_3
[2] Total Inorganic Carbon, CO_2+HCO_3^-+CO_3^{2-}
[3] Total Ammonia Nitrogen in solid ammonium bicarbonate after precipitation
[4] Error in sample preparation

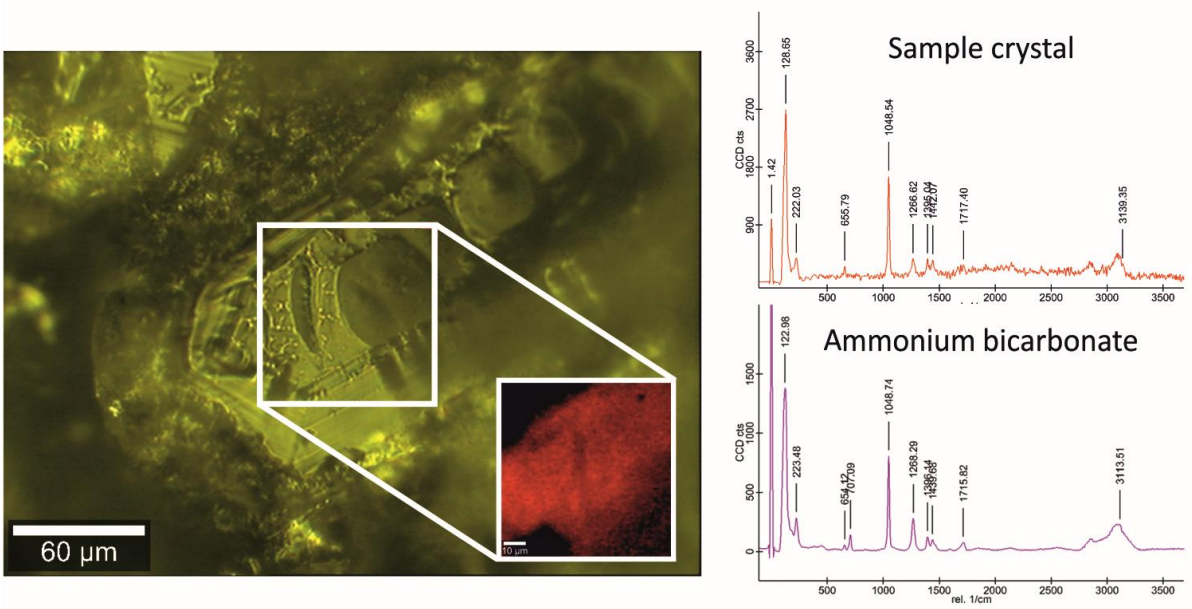

Figure 4. Solid crystals. Crystals were identified as pure ammonium bicarbonate by Raman spectroscopy.

Ammonium bicarbonate can precipitate if there are favourable conditions for nucleation under supersaturation [39]. For cooled concentrates, supersaturation cannot currently be modelled as the solubility constant of ammonium bicarbonate has not been defined at temperatures below 0°C, and the salt effect (diminishing activities due to competing ions) is significant.

To evaluate limits for saturation conditions, ionic strength (IS), ammonium bicarbonate ionic strength (IS_{ABC}), the ratio of these two (IS_{ABC}/IS), and ammonium bicarbonate ionic product (IP_{ABC}) are compared (See Figure 5 and Table 3). These variables are calculated from measured concentrations.

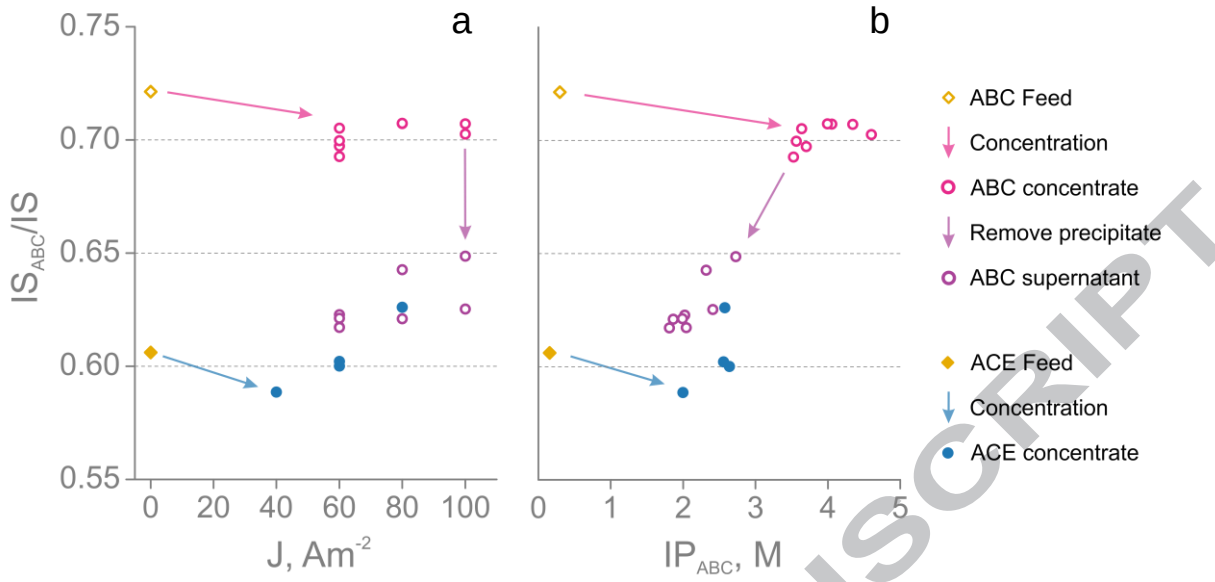

Figure 5. Relative ammonium bicarbonate ionic strength. Presented in relation to (a) current density and (b) ionic strength, for feeds, concentrates and precipitation supernatants. When feeds are concentrated, IS_{ABC}/IS remains on a similar level to feed and ionic strength increases. Precipitation at -18°C for ABC feed decreases IS_{ABC}/IS to a similar level found at ACE feed.

As concentrate from ABC feed is cooled, precipitation occurred in all ABC concentrate samples and a residual ABC supernatant can be expected to be close to saturation conditions of solid ammonium bicarbonate. We examined the statistics of different liquids, namely ACE concentrate, ABC concentrate and ABC supernatant to find relevant differences. Averages of both IP_{ABC} and IS_{ABC} were higher for ACE concentrate than ABC supernatant (2.44 M^2 and 2.15 M^2, and 1.58 M and 1.47 M, respectively), suggesting a more saturated solution. However, no precipitation was detected in ACE concentrates. As competing ions can lower the activities of precipitating ions, we then looked at the relative ionic strength of ammonium bicarbonate (IS_{ABC}/IS). The average IS_{ABC}/IS was lower for ACE concentrate compared to ABC supernatant (60 % and 63 %, respectively). Otherwise the samples from ABC supernatant and ACE concentrate have similar ionic properties. One-way ANOVA for IS_{ABC}, IP_{ABC} and IS_{ABC}/IS between ABC supernatant and ACE concentrate gives p-values of 0.05, 0.15 and 0.02, respectively, implicating weak or no statistical difference when using a 5 % confidence interval. ABC supernatant and ACE concentrate as a combined group however differ very significantly from supersaturated ABC concentrate (one-way ANOVA for IS_{ABC}, IP_{ABC} and IS_{ABC}/IS between combined ABC supernatant and ACE concentrate and ABC concentrate gives p-values of $2.9 \cdot 10^{-8}$, $4.8 \cdot 10^{-9}$ and $8.6 \cdot 10^{-11}$, respectively, indicating significant difference using a 5% confidence interval). These results indicate that both ABC supernatant and ACE concentrate are close to saturation, while ABC concentrate is supersaturated. The limiting conditions for forming a solid precipitate in this experiment occur close to the conditions measured for ABC supernatant and ACE concentrate, towards the conditions found in ABC concentrate. In separate short term experiments with concentrate feed recycled to the feed (data not presented), trace amounts of ammonium bicarbonate precipitate has been successfully collected also when using ACE feed in a concentrate with similar composition to the ACE concentrate shown here, further supporting that the notion that ACE concentrate is close to saturation (at -18°C).

Table 3. Average parameters of liquids. Ionic strength (IP), ammonium bicarbonate ionic strength (IP_{ABC}), and ammonium bicarbonate ionic product (IP_{ABC}) of ACE and ABC feed, their concentrates and ABC supernatant after precipitation. N = number of parallel experiments. If multiple experiments, values are averages with 95 % confidence intervals.

		N	IS, M	IS_{ABC}, M	IP_{ABC}, M^2	IS_{ABC}/IS, %
ACE	**Feed**	1	0.69	0.42	0.15	60.9
	Concentrate	4	2.67±0.19	1.61±0.14	2.44±0.48	60.4±2.5
ABC	**Feed**	1	0.75	0.54	0.30	72.1
	Concentrate	8	2.83±0.11	1.99±0.08	3.93±0.33	70.2±0.5
	Supernatant	8	2.35±0.11	1.47±0.09	2.15±0.26	62.7±1.0

From these data sets, we can thus hypothesise that to reach precipitation of ammonium bicarbonate from concentrated urine at -18°C, minimum threshold values for both IP_{ABC} and IS_{ABC}/IS must be satisfied. These values are estimated at around 2.25 M^2 for IP_{ABC} and ~62% for IS_{ABC}/IS, these being combined averages for ABC supernatant and ACE concentrate from our experiments.

These results suggest that the limiting factor for further precipitation is the relative ammonium bicarbonate concentration to the total ionic strength. This means that other ions in the concentrate block further precipitation and to reach higher capture through precipitation, alternate ways of ion separation are required.

3.3 Feasibility of nitrogen capture through electro-concentration

The energy used for electro-concentration was measured by the potentiostat as an integrated product of applied potential and resulting current. The system produced oxygen at the anode and hydrogen on the cathode with applied total cell voltages of 3 to 5 V, depending on the current density. Specific electrical energy consumption was measured as 30, 35±1 and 46 MJ kg N^{-1} for ACE feed at 40, 60 and 80 A m^{-2}, and 35±1, 39±2 and 47±3 MJ kg N^{-1} for ABC feed at 60, 80 and 100 A m^{-2}, respectively. This energy consumption is high compared to bio-electroconcentration systems applying bioanodes running on urine (8.6 MJ/kg N [25], and 4.9 MJ/kg N [40]). The use of bioanodes and oxygen reducing cathodes holds promise to reach current densities similar to those used in this study [4,25] with significantly lower energy demands, potentially even reaching positive energy outputs [4,41].

Capture of nitrogen as solid ammonium bicarbonate without chemical addition by cooling the concentrate is found possible for ABC feed (simulated ureolysed and digested feed) reaching up to 17 % capture. The ACE feed (simulated ureolysed feed) did not show capacity for capture as solid via cooling due to low IP_{ABC}/IS ratio. Limited methods are available to increase the portion that can be captured as solid due to the large concentrations of competing ions, especially sodium, potassium and chloride. Concentrate refeeding or serial reactor systems can be applied to the concentrate to reach higher concentrations and liquid capture rates. However, these methods will not significantly change the total fraction of nitrogen that can be captured as solid ammonium bicarbonate as they don't remove competing ions which will also concentrate, further inhibiting ammonium bicarbonate precipitation (for more detailed evaluation of competitive ion transport, see Thompson Brewster et al. 2017). This limitation renders capture by cooling non-feasible as a primary means of nitrogen separation from the concentrate in the studied settings. Selective membranes or other methods of removing competing salts could change this conclusion and could enable precipitation by cooling as a viable option. For specific ammonium bicarbonate removal, other methods such as thermal evaporation or stripping are seen more appropriate as ammonium and bicarbonate are the only readily evaporative species.

Acknowledgements

The authors acknowledge the facilities, and the scientific and technical assistance of the Analytical Services Laboratory at the Advanced Water Management Centre, The University of Queensland and Dr B. C. Donose for help with the spectroscopic analyses. This work was performed in part at the Queensland node of the Australian National Fabrication Facility, a company established under the National Collaborative Research Infrastructure Strategy to provide nano and microfabrication facilities for Australia's researchers.

Funding

This research was supported financially by Maj and Tor Nessling foundation and Walter Ahlström foundation supporting Johannes Jermakka; and the Australian Research Council Project LP 150100402 in partnership with Queensland Urban Utilities (QUU) and ABR Process Development; the Australian Grain Research & Development Corporation Grain Research Scholarship (GRS10661) supporting Emma Thompson Brewster. Pablo Ledezma acknowledges an ECR Development Fellowship from The University of Queensland.

Referee suggestions

Dr. Kai Udert, EAWAG, Switzerland. Email: kai.udert@eawag.ch
Dr. Srikanth Mutnuri, BIRLA Institute, India. Email: srikanth@goa.bits-pilani.ac.in
Dr. Leiyu Feng, Tongji University, China. Email: leiyufeng@tongji.edu.cn

References

[1] T.A. Larsen, K.M. Udert, J. Lienert, Source separation and decentralization for wastewater management, IWA, London, 2013.

[2] J. Rockström, W. Steffen, K. Noone, Å. Persson, F.S. Chapin, E. Lambin, T.M. Lenton, M. Scheffer, C. Folke, H.J. Schellnhuber, B. Nykvist, C.A. de Wit, T. Hughes, S. van der Leeuw, H. Rodhe, S. Sörlin, P.K. Snyder, R. Costanza, U. Svedin, M. Falkenmark, L. Karlberg, R.W. Corell, V.J. Fabry, J. Hansen, B. Walker, D. Liverman, K. Richardson, P. Crutzen, J. Foley, Planetary boundaries: Exploring the safe operating space for humanity, Ecol. Soc. 14 (2009). doi:10.1038/461472a.

[3] E. Friedler, D. Butler, Y. Alfiya, Wastewater composition, in: T.A. Larsen, K.M. Udert, J. Lienert (Eds.), Source Sep. Decentralization Wastewater Manag., IWA Publishing, Oxford, 2013: pp. 241–258.

[4] P. Ledezma, P. Kuntke, C.J.N. Buisman, J. Keller, S. Freguia, Source-separated urine opens golden opportunities for microbial electrochemical technologies, Trends Biotechnol. 33 (2015) 214–220. doi:10.1016/j.tibtech.2015.01.007.

[5] H. Jönsson, B. Vinnerås, Closing the loop: Recycling nutrients to agriculture, in: T.A. Larsen, K.M. Udert, J. Lienert (Eds.), Source Sep. Decentralization Wastewater Manag., IWA Publishing, Oxford, 2013: pp. 163–178.

[6] T.A. Larsen, K.M. Udert, J. Lienert, Editorial, in: T.A. Larsen, K.M. Udert, J. Lienert (Eds.), Source Sep. Decentralization Wastewater Manag., IWA Publishing, Oxford, 2013: pp. 1–11.

[7] M. Maurer, W. Pronk, T.A. Larsen, Treatment processes for source-separated urine, Water Res. 40 (2006) 3151–3166. doi:10.1016/j.watres.2006.07.012.

[8] S. Antonini, S. Paris, T. Eichert, J. Clemens, Nitrogen and Phosphorus Recovery from Human Urine by Struvite Precipitation and Air Stripping in Vietnam, Clean - Soil, Air, Water. 39 (2011) 1099–1104. doi:10.1002/clen.201100036.

[9] B. Etter, E. Tilley, R. Khadka, K.M. Udert, Low-cost struvite production using source-separated urine in Nepal, Water Res. 45 (2011) 852–862. doi:10.1016/j.watres.2010.10.007.

[10] A. Hug, K.M. Udert, Struvite precipitation from urine with electrochemical magnesium dosage, Water Res. 47 (2013) 289–299. doi:10.1016/j.watres.2012.09.036.

[11] J.A. Wilsenach, C.A. Schuurbiers, M.C. van Loosdrecht, Phosphate and potassium recovery from source separated urine through struvite precipitation, Water Res. 41 (2007) 458–466. doi:10.1016/j.watres.2006.10.014.

[12] T. Duong, Z.L. Xie, D. Ng, M. Hoang, Ammonia removal from aqueous solution by membrane distillation, Water Environ. J. 27 (2013) 425–434. doi:DOI 10.1111/j.1747-6593.2012.00364.x.

[13] A. Zarebska, K.V. Christensen, B. Norddahl, The Application of Membrane Contactors for Ammonia Recovery from Pig Slurry, Procedia Eng. 44 (2012) 1642–1645. doi:10.1016/j.proeng.2012.08.895.

[14] M. Ronteltap, M. Maurer, W. Gujer, Struvite precipitation thermodynamics in source-separated urine, Water Res. 41 (2007) 977–984. doi:10.1016/j.watres.2006.11.046.

[15] M. Rodriguez Arredondo, P. Kuntke, A. ter Heijne, H.V.M. Hamelers, C.J.N. Buisman, Load ratio determines the ammonia recovery and energy input of an electrochemical system, Submitted. 111 (2017) 330–337. doi:10.1016/j.watres.2016.12.051.

[16] P. Kuntke, M. Rodriguez Arredondo, L. Widyakristi, A. Ter Heijne, T.H.J.A. Sleutels, H.V.M. Hamelers, C.J.N. Buisman, Hydrogen gas recycling for energy efficient ammonia recovery in electrochemical systems, Environ. Sci. Technol. (2017) acs.est.6b06097. doi:10.1021/acs.est.6b06097.

[17] A.K. Luther, J. Desloover, D.E. Fennell, K. Rabaey, Electrochemically driven extraction and recovery of ammonia from human urine, Water Res. 87 (2015) 367–377. doi:10.1016/j.watres.2015.09.041.

[18] J. Desloover, A. Abate Woldeyohannis, W. Verstraete, N. Boon, K. Rabaey, Electrochemical resource recovery from digestate to prevent ammonia toxicity during anaerobic digestion, Environ. Sci. Technol. 46 (2012) 12209–12216. doi:10.1021/es3028154.

[19] J. Desloover, J. De Vrieze, M. Van De Vijver, J. Mortelmans, R. Rozendal, K. Rabaey, Electrochemical nutrient recovery enables ammonia toxicity control and biogas desulfurization in anaerobic digestion, Environ. Sci. Technol. 49 (2015) 948–955. doi:10.1021/es504811a.

[20] P. Kuntke, Nutrient and energy recovery from urine, PhD Thesis, 2013. http://edepot.wur.nl/254782.

[21] M. Rodríguez Arredondo, P. Kuntke, a. W. Jeremiasse, T.H.J. a. Sleutels, C.J.N. Buisman, a. ter Heijne, Bioelectrochemical systems for nitrogen removal and recovery from wastewater, R. Soc. Chem. 2015. 1 (2014) 22–33. doi:10.1039/C4EW00066H.

[22] S. Gildemyn, A.K. Luther, S.J. Andersen, J. Desloover, K. Rabaey, Electrochemically and bioelectrochemically induced ammonium recovery, J. Vis. Exp. (2015). doi:10.3791/52405.

[23] P. Kuntke, P. Zamora, M. Saakes, C.J.N. Buisman, H.V.M. Hamelers, Gas-permeable hydrophobic tubular membranes for ammonia recovery in bio-electrochemical systems, Environ. Sci. Water Res. Technol. (2016). doi:10.1039/c5ew00299k.

[24] R.C. Tice, Y. Kim, Energy efficient reconcentration of diluted human urine using ion exchange membranes in bioelectrochemical systems, Water Res. 64 (2014) 61–72. doi:10.1016/j.watres.2014.06.037.

[25] P. Ledezma, J. Jermakka, J. Keller, S. Freguia, Recovering Nitrogen as a Solid without Chemical Dosing: Bio-Electroconcentration for Recovery of Nutrients from Urine, Environ. Sci. Technol. Lett. (2017) acs.estlett.7b00024. doi:10.1021/acs.estlett.7b00024.

[26] W. Pronk, M. Biebow, M. Boller, Treatment of source-separated urine by a combination of bipolar electrodialysis and a gas transfer membrane, Water Sci. Technol. 53 (2006) 139–146. doi:10.2166/wst.2006.086.

[27] W. Pronk, S. Zuleeg, J. Lienert, B. Escher, M. Koller, A. Berner, G. Koch, M. Boller, Pilot experiments with electrodialysis and ozonation for the production of a fertiliser from urine, Water Sci. Technol. 56 (2007) 219–227. doi:10.2166/wst.2007.575.

[28] M. Mondor, L. Masse, D. Ippersiel, F. Lamarche, D.I. Massé, Use of electrodialysis and reverse osmosis for the recovery and concentration of ammonia from swine manure, Bioresour. Technol. 99 (2008) 7363–7368. doi:http://dx.doi.org/10.1016/j.biortech.2006.12.039.

[29] D. Ippersiel, M. Mondor, F. Lamarche, F. Tremblay, J. Dubreuil, L. Masse, Nitrogen potential recovery and concentration of ammonia from swine manure using electrodialysis coupled with air stripping, J. Environ. Manage. 95 (2012) S165–S169. doi:DOI 10.1016/j.jenvman.2011.05.026.

[30] E. Thompson Brewster, J. Jermakka, S. Freguia, D.J. Batstone, Modelling recovery of ammonium from urine by electro-concentration in a 3-chamber cell, Water Res. (2017). doi:10.1016/j.watres.2017.07.043.

[31] W.M. Haynes, CRC Handbook of Chemistry and Physics. 92nd Edition, Greece, 2012.

[32] K. Xu, J. Li, M. Zheng, C. Zhang, T. Xie, C. Wang, The precipitation of magnesium potassium phosphate hexahydrate for P and K recovery from synthetic urine, Water Res. 80 (2015) 71–79. doi:10.1016/j.watres.2015.05.026.

[33] K.M. Udert, T.A. Larsen, W. Gujer, Fate of major compounds in source-separated urine, Water Sci. Technol. 54 (2006) 413–420. doi:10.2166/wst.2006.921.

[34] K.M. Udert, T.A. Larsen, M. Biebow, W. Gujer, Urea hydrolysis and precipitation dynamics in a urine-collecting system, Water Res. 37 (2003) 2571–2582. doi:http://dx.doi.org/10.1016/S0043-1354(03)00065-4.

[35] K. Solon, X. Flores-Alsina, C.K. Mbamba, E.I.P. Volcke, S. Tait, D. Batstone, K. V. Gernaey, U. Jeppsson, Effects of ionic strength and ion pairing on (plant-wide) modelling of anaerobic digestion, Water Res. 70 (2015) 235–245. doi:10.1016/j.watres.2014.11.035.

[36] P. Atkins, J. de Paula, Physical Chemistry, W. H. Freeman, 2006. https://books.google.fi/books?id=lk2PzH9LmS8C.

[37] H. Strathmann, Ion-exchange membrane separation processes, in: S. Heiner (Ed.), Membr. Sci. Technol., Elsevier, 2004: pp. v–vi. doi:http://dx.doi.org/10.1016/S0927-5193(04)80031-7.

[38] W. Pronk, M. Biebow, M. Boller, Electrodialysis for recovering salts from a urine solution containing micropollutants, Environ. Sci. Technol. 40 (2006) 2414–2420. doi:10.1021/es051921i.

[39] J.I. Kroschwitz, A. Seidel, Kirk-Othmer encyclopedia of chemical technology, Wiley-Interscience, Hoboken, N.J, 2004.

[40] P. Zamora, T. Georgieva, A. Ter Heijne, T. Sleutels, A. Jeremiasse, Ammonia recovery from urine in a scaled-up Microbial Electrolysis Cell, (2017) 1–9. doi:10.1016/j.jpowsour.2017.02.089.

[41] P. Kuntke, K.M. Smiech, H. Bruning, G. Zeeman, M. Saakes, T.H.J.A. Sleutels, H.V.M. Hamelers, C.J.N. Buisman, K.M. Śmiech, H. Bruning, G. Zeeman, M. Saakes, T.H.J.A. Sleutels, H.V.M. Hamelers, C.J.N. Buisman, Ammonium recovery and energy production from urine by a microbial fuel cell, Water Res. 46 (2012) 2627–2636. doi:10.1016/j.watres.2012.02.025.

Graphical abstract

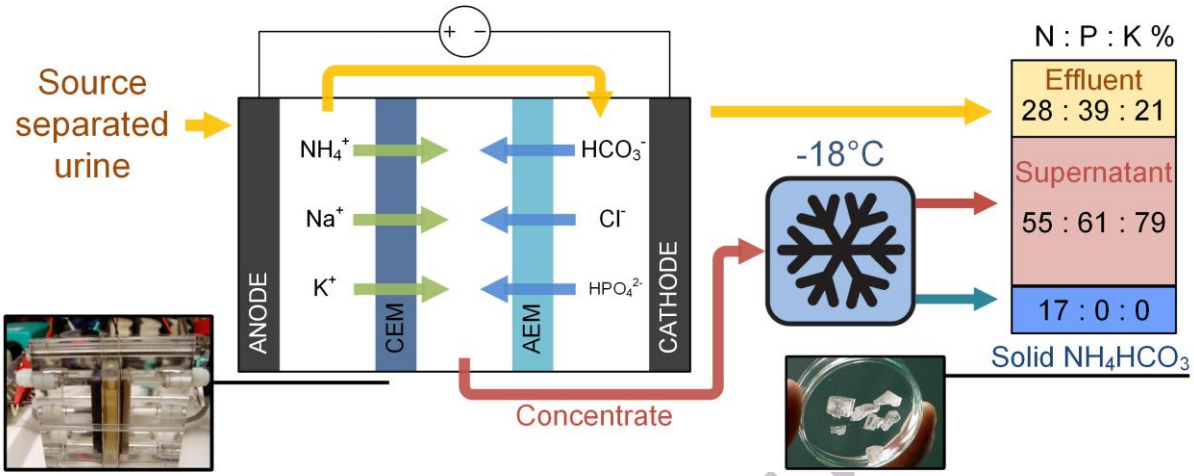

Highlights for the manuscript titled: "Electro-concentration for chemical-free nitrogen capture as solid ammonium bicarbonate" by Jermakka, Thompson Brewster, Ledezma and Freguia

- Simulated source-separated urine was electro-concentrated for nutrient recovery
- 72 % of nitrogen was captured, 17 % of which as solid ammonium bicarbonate crystals
- Limiting parameters were established for chemical free nitrogen capture as a solid